Numerical anlysis of Soret-Dufour, Radiation and chemical reaction effects on Unsteady MHD flow of Viscoelastic Dusty fluid over Inclined Porous Plate

[1]N. Pandya, [2]Ravi Kant Yadav*, [3]A. K. Shukla
[1]Assistant Professor, [2]Research Scholar, [3]Assistant Professor
[1,2] Department of Mathematics & Astronomy, University of Lucknow, Lucknow, India.
[3]Department of Mathematics RSKD PG College, Jaunpur, India

Abstract : This article addresses the effect of Radiation and chemical reaction on Unsteady MHD flow of Viscoelastic Dusty fluid over inclined porous plate. Simultaneous study of heat and mass transfer is performed by considering Soret and Dufour effects. No-slip conditions for velocity, temperature and concentration are imposed. The non dimensional governing non-linear partial differential equations are solved numerically using Crank-Nicolson implicit finite difference method. Changes in velocity, temperature and concentration are explained graphically for different values physical parameter. Skin friction coefficient, Nusselt number and Sherwood number are analysed with help of tables.

IndexTerms **- Free convection, MHD flow, Dusty fluid, Viscoelastic fluid, Radiation effect, Chemical reaction, Heat and Mass transfer, Soret-Dufour effect, Crank-Nicolson finite difference method.**

I. INTRODUCTION

The study of viscoelastic fluid flowing over inclined surfaces embedded in porous media in presence of magnetic field has attracted the scientists because of its application in geophysics, astrophysics, geo- hydrology, chemical engineering, biological system, soil physics and filtration of solids from liquids.

Many researchers have studied the transient laminar natural convection flow past a vertical porous plate for the application in the branch of science and technology such as in the field of agriculture engineering and chemical engineering. In petroleum refineries, movement of oil, water and gas through porous media for purification and filtration are bright applied areas of research.

Walters and Beard [1] studied the boundary layer analysis of idealized viscoelastic fluid . Dash et al. [2] analysed mass and heat transfer effect on MHD flow of a viscoelastic fluid through porous medium with oscillatory suction and heat source. Gorla and Singh [3] carried out the boundary layer analysis of free convective flow of conducting Newtonian fluid over an infinite vertical porous plate. Metri et al. [4] developed a numerical model to investigate the MHD mixed convective boundary layer viscoelastic fluid flow over a stretching sheet embedded in a porous medium in the presence of viscous dissipation. Sharma et al. [5] led an research of Heat and mass Transfer effects on unsteady MHD natural convection flow of a chemically reactive and radiating fluid through a Porous medium past a moving vertical plate with arbitrary ramped temperature.

Cortell [6] studied the viscoelastic fluid flow and heat transfer over a stretching sheet. Frater [8] has analysed the effect of the elasticity of the fluid on the steady streaming produced by an oscillating cylinder. Chang [7] made a theoretical study of the problem using Walters liquid B' as model for viscoelastic fluid. N. pandya and A. K. Shukla [9] led an investigation on effect of radiation and chemical reaction on an unsteady Walter's-B viscoelastic MHD flow past a vertical porous plate.

the aim of this article is to investigate the Soret- Dufour, radiation and chemical reaction effects on natural convection heat and mass transfer of viscoelastic fluid over a fixed inclined porous plate embedded in porous medium. Non dimensional form of governing non linear partial equations of flow variables are solved numerically using Crank-Nicolson implicit finite difference method. Velocity, temperature and concentration profiles are discussed with help of graphs and skin friction coefficient, Nusselt number and Sherwood number are discussed with help of tables.

II. MATHEMATICAL ANALYSIS

The unsteady free convective flow of a viscoelastic fluid (Walter's-B model) past an infinite inclined porous plate embedded in a porous medium and permeability in presence of a transverse magnetic field is considered. Let us consider x'-axis be along the plate in the direction of the flow, y'-axis normal to it, z'-axis is normal to x'y' plane and the magnetic Reynolds number is much less than unity so that the induced magnetic field is neglected in comparison with the applied transverse magnetic field, Cowling[10]. The basic flow in the medium is, therefore, entirely due to the buoyancy force caused by the temperature difference between the wall and the medium. It is assumed that initially, at $t \le 0$ the plate as well as fluid are at the same temperature and also concentration of the species is very low so that the Soret and Dufour effects are neglected. When t'>0, the temperature of the plate is instantaneously raised to $T_w^{'}$ and the concentration of the species is set to $C_w^{'}$. Because of infinite length in x' direction, flow variables are function of t' and y' only. Under usual Boussinesq approximation, governing equations of this model are given by

$$H_x^{'} = \frac{\sigma B_0}{1+m^2}(mu'-w')$$
$$H_z^{'} = \frac{\sigma B_0}{1+m^2}(u'+mw') \quad (1)$$

where u' and w' are velocities, H'_x and H'_z are electric current density along x'-axis and z'-axis respectively, m is Hall parameter. Because of infinite length in x' direction, flow variables are function of t' and y' only. Under usual Boussinesq approximation, governing equations of this model are given by:

$$\frac{\partial v'}{\partial y'} = 0 \Rightarrow v' = -v_0 (const) \quad (2)$$

$$\frac{\partial u'}{\partial t'} + v'\frac{\partial u'}{\partial y'} = \nu \frac{\partial^2 u'}{\partial y'^2} - \nu_1 \frac{\partial^3 u'}{\partial y'^2 \partial t'} + g\beta(T'-T'_\infty)\cos(\alpha) + g\beta^*(C'-C'_\infty)\cos(\alpha)$$
$$-\frac{\sigma B_0^{\,2}}{\rho(1+m^2)}(u'+mw') - \frac{\nu u'}{K'} + \frac{KN_0}{\rho}(u'_d - u') \quad (3)$$

$$\frac{\partial w'}{\partial t'} + v'\frac{\partial w'}{\partial y'} = \nu \frac{\partial^2 w'}{\partial y'^2} - \nu_1 \frac{\partial^3 w'}{\partial y'^2 \partial t'}$$
$$+\frac{\sigma B_0^{\,2}}{\rho(1+m^2)}(mu'-w') - \frac{\nu w'}{K'} + \frac{KN_0}{\rho}(w'_d - w') \quad (4)$$

$$m_1 \frac{\partial u'_d}{\partial t'} = F_d(u'-u'_d) \quad (5)$$

$$m_1 \frac{\partial w'_d}{\partial t'} = F_d(w'-w'_d) \quad (6)$$

$$\rho c_p \left(\frac{\partial T'}{\partial t'} + v'\frac{\partial T'}{\partial y'} \right) = k\frac{\partial^2 T'}{\partial y'^2} - \frac{\partial q_r}{\partial y'} + \frac{\rho D_m K_T}{c_s}\frac{\partial^2 C'}{\partial y'^2} \quad (7)$$

$$\frac{\partial C'}{\partial t'} + v'\frac{\partial C'}{\partial y'} = D_m \frac{\partial^2 C'}{\partial y'^2} + \frac{D_m K_T}{T_m}\frac{\partial^2 T'}{\partial y'^2} - k_r(C' - C'_\infty) \quad (8)$$

and boundary and initial conditional for this flow problem are given as

$$t' \le 0 \quad u'=0 \quad w'=0 \quad u'_d=0 \quad w'_d=0 \quad T'=T'_\infty \quad C'=C'_\infty \quad \forall y'$$
$$t'>0 \quad u'=u_0 \quad w'=0 \quad u'_d=u_0 \quad w'_d=0 \quad T'=T'_\infty+(T'_w-T'_\infty)e^{-At'}$$
$$C'=C'_\infty+(C'_w-C'_\infty)e^{-At'} \quad at \; y'=0$$
$$u'=0 \quad w'=0 \quad u'_d=0 \quad w'_d=0 \quad T'\to T'_\infty \quad C'\to C'_\infty \quad y'\to\infty \quad (9)$$

Where $T_w^{'}$ and $C_w^{'}$ are concentration and temperature respectively of plate, $A=\frac{v_0^2}{\nu}$, $u_d^{'}$ and $w_d^{'}$ are component of velocity of dust particles along x' and y' directions respectively, K_r is chemical reaction parameter, F_d is the stoke's resistance coefficient, ν_1 is viscoelasticityis the number density of the dust N_0 particles which is constant m_1 is the mass of dust particles, K is the proportionality constant, β^* is

coefficient of volume expansion for mass transfer, β is volumetric coefficient of thermal expansion, v' is velocity along y'-axis, σ is electrical conductivity, D_m is molecular diffusivity, 'g' is acceleration due to gravity, K_T is thermal diffusion ratio, ρ is fluid density, k is thermal conductivity of fluid, C' and T' are dimensional concentration and temperature, C'_∞ and T'_∞ are concentration and temperature of free stream, c_p is specific heat at constant pressure, q_r is radiative heat along y'-axis, ν is kinematic viscosity and T_m is mean fluid temperature.

The radiative heat flux term by using Roseland approximation is given by

$$q_r = -\frac{4\sigma}{3k_m}\frac{\partial T'^4}{\partial y'} \tag{10}$$

where σ and k_m are Stefan Boltzmann constant and mean absorption coefficient respectively. in this problem temperature difference within flow is sufficiently small, so that T^4 may be expressed linearly with temperature. It is observed by expanding in a Taylor's series about T'_∞ and neglecting higher order term, thus

$$T'^4 \cong 4T'^3_\infty T' - 3T'^4_\infty \tag{11}$$

Using equations 10 and 11, equation 7 takes the form

$$\rho c_p\left(\frac{\partial T'}{\partial t'} + v'\frac{\partial T'}{\partial y'}\right) = k\frac{\partial^2 T'}{\partial y'^2} + \frac{16\sigma T'^3_\infty}{3k_m}\frac{\partial^2 T'}{\partial y'^2} + \frac{\rho D_m K_T}{c_s}\frac{\partial^2 C'}{\partial y'^2} \tag{12}$$

Now in order to obtain non-dimensional partial differential equations, we are introducing following dimensionless variables and constants.

$$u = \frac{u'}{u_0},\quad t = \frac{t'v_0^2}{\nu},\quad \theta = \frac{T'-T'_\infty}{T'_w - T'_\infty},$$

$$C = \frac{C'-C'_\infty}{C'_w - C'_\infty},\quad Gm = \frac{\nu g\beta^*(C'_w - C'_\infty)}{u_0 v_0^2}$$

$$Gr = \frac{\nu g\beta(T'_w - T'_\infty)}{u_0 v_0^2},\quad Du = \frac{D_m K_T(C'_w - C'_\infty)}{c_s c_p \nu(T'_w - T'_\infty)},$$

$$Sr = \frac{D_m K_T(T'_w - T'_\infty)}{T_m \nu(C'_w - C'_\infty)}$$

$$K = \frac{v_0^2 K'}{\nu^2},\quad \Pr = \frac{\mu c_p}{k},\quad M = \frac{\sigma B_0^2 \nu}{\rho v_0^2},$$

$$R = \frac{4\sigma T'^3_\infty}{k_m k},\quad Sc = \frac{\nu}{D_m}, \Gamma = \frac{v_0^2 \nu_1}{\nu^2}$$

$$y = \frac{y'v_0}{\nu},\quad w = \frac{w'}{u_0},\quad u_d = \frac{u'_d}{u_0},$$

$$w_d = \frac{w'_d}{u_0},\quad B = \frac{\nu F_d N_0}{\rho u_0^2},\quad B_1 = \frac{m_1 v_0^2}{\nu F_d}, K_r = \frac{k_r \nu}{v_0^2} \tag{13}$$

By introducing above dimensionless variables and constants the Equations 3-6, 8 and 12 converted as follows

$$\frac{\partial u}{\partial t}-\frac{\partial u}{\partial y}=\frac{\partial^2 u}{\partial y^2}-\Gamma\frac{\partial^3 u}{\partial y^2\partial t}+GrCos(\alpha)\theta+GmCos(\alpha)C+B_1(u_d-u)-\left(\frac{M}{1+m^2}+\frac{1}{K}\right)u-\left(\frac{mM}{1+m^2}\right)w \quad (14)$$

$$\frac{\partial w}{\partial t}-\frac{\partial w}{\partial y}=\frac{\partial^2 w}{\partial y^2}-\Gamma\frac{\partial^3 w}{\partial y^2\partial t}+B_1(w_d-w)-\left(\frac{M}{1+m^2}+\frac{1}{K}\right)w+\left(\frac{mM}{1+m^2}\right)u \quad (15)$$

$$B\frac{\partial u_d}{\partial t}=u-u_d \quad (16)$$

$$B\frac{\partial w_d}{\partial t}=w-w_d \quad (17)$$

$$\frac{\partial \theta}{\partial t}-\frac{\partial \theta}{\partial y}=\frac{1}{\Pr}\left(1+\frac{4R}{3}\right)\frac{\partial^2\theta}{\partial y^2}+Du\frac{\partial^2 C}{\partial y^2} \quad (18)$$

$$\frac{\partial C}{\partial t}-\frac{\partial C}{\partial y}=\frac{1}{Sc}\frac{\partial^2 C}{\partial y^2}+Sr\frac{\partial^2\theta}{\partial y^2}-K_rC \quad (19)$$

non dimensional boundary and initial conditions are:

$$t\le 0 \quad u=0 \;\; w=0 \;\; u_d=0 \;\; w_d=0 \;\; \theta=0 \;\; C=0 \quad \forall y$$

$$t>0 \;\; u=0 \;\; w=0 \;\; u_d=0 \;\; w_d=0 \;\; \theta=e^{-t} \;\; C=e^{-t} \quad at \;\; y=0 \quad (20)$$

$$u=0 \;\; w=0 \;\; u_d=0 \;\; w_d=0 \;\; \theta\to 0 \;\; C\to 0 \quad y\to\infty$$

The parameters of engineering interest for the present problem are the skin friction coefficient τ_1 and τ_2, local Nusselt number *Nu* and Sherwood number *Sh* which indicate physically the wall shear stress, the rate of heat transfer and the local surface mass flux respectively. The dimensionless skin-friction coefficient, Nusselt number and Sherwood number for impulsively started plate are given by :

$$\tau_1=\left(\frac{\partial u}{\partial y}\right)_{y=0}$$

$$\tau_2=\left(\frac{\partial w}{\partial y}\right)_{y=0} \quad (21)$$

$$Nu=-\left(\frac{\partial \theta}{\partial y}\right)_{y=0}$$

$$Sh=-\left(\frac{\partial C}{\partial y}\right)_{y=0}$$

.

III. METHOD OF SOLUTION

The unsteady nonlinear system of partial differential equations 14-19 with conditions equation-20 are solved by using Crank-Nicolson implicit finite-difference scheme. Consider a rectangular region with y varying from 0 to y max (= 4), where y max corresponds to $y=\infty$ at which lies well outside the momentum and energy boundary layers. According to Crank- finite-difference equations corresponding to 14-19 are given by

$$\frac{u_{i,j+1}-u_{i,j}}{\Delta t}-\frac{u_{i+1,j}-u_{i,j}}{\Delta y}=\left(\frac{u_{i-1,j}-2u_{i,j}+u_{i+1,j}+u_{i-1,j+1}-2u_{i,j+1}+u_{i+1,j+1}}{2(\Delta y)^2}\right)$$
$$-\Gamma\left(\frac{u_{i-1,j}-2u_{i,j}+u_{i+1,j}+u_{i-1,j+1}-2u_{i,j+1}+u_{i+1,j+1}}{2(\Delta y)^2\,\Delta t}\right)+B_1\left(\left(\frac{(u_d)_{i,j+1}+(u_d)_{i,j}}{2}\right)-\left(\frac{u_{i,j+1}+u_{i,j}}{2}\right)\right)$$
$$+Gr\cos(\alpha)\left(\frac{\theta_{i,j+1}+\theta_{i,j}}{2}\right)+Gr\cos(\alpha)\left(\frac{C_{i,j+1}+C_{i,j}}{2}\right)-\left(\frac{M}{1+m^2}+\frac{1}{K}\right)\left(\frac{u_{i,j+1}+u_{i,j}}{2}\right)-\left(\frac{mM}{1+m^2}\right)\left(\frac{w_{i,j+1}+w_{i,j}}{2}\right) \quad (22)$$

$$\frac{w_{i,j+1}-w_{i,j}}{\Delta t}-\frac{w_{i+1,j}-w_{i,j}}{\Delta y}=\left(\frac{w_{i-1,j}-2w_{i,j}+w_{i+1,j}+w_{i-1,j+1}-2w_{i,j+1}+w_{i+1,j+1}}{2(\Delta y)^2}\right)$$
$$-\Gamma\left(\frac{w_{i-1,j}-2w_{i,j}+w_{i+1,j}+w_{i-1,j+1}-2w_{i,j+1}+w_{i+1,j+1}}{2(\Delta y)^2\,\Delta t}\right)+B_1\left(\left(\frac{(w_d)_{i,j+1}+(w_d)_{i,j}}{2}\right)-\left(\frac{w_{i,j+1}+w_{i,j}}{2}\right)\right)$$
$$-\left(\frac{M}{1+m^2}+\frac{1}{K}\right)\left(\frac{w_{i,j+1}+w_{i,j}}{2}\right)+\left(\frac{mM}{1+m^2}\right)\left(\frac{u_{i,j+1}+u_{i,j}}{2}\right) \quad (23)$$

$$B\left(\frac{(u_d)_{i,j+1}-(u_d)_{i,j}}{\Delta t}\right)=\left(\left(\frac{u_{i,j+1}+u_{i,j}}{2}\right)-\left(\frac{(u_d)_{i,j+1}+(u_d)_{i,j}}{2}\right)\right) \quad (24)$$

$$B\left(\frac{(w_d)_{i,j+1}-(w_d)_{i,j}}{\Delta t}\right)=\left(\left(\frac{w_{i,j+1}+w_{i,j}}{2}\right)-\left(\frac{(w_d)_{i,j+1}+(w_d)_{i,j}}{2}\right)\right) \quad (25)$$

$$\frac{\theta_{i,j+1}-\theta_{i,j}}{\Delta t}-\frac{\theta_{i+1,j}-\theta_{i,j}}{\Delta y}=\frac{1}{\Pr}\left(1+\frac{4R}{3}\right)\left(\frac{\theta_{i-1,j}-2\theta_{i,j}+\theta_{i+1,j}+\theta_{i-1,j+1}-2\theta_{i,j+1}+\theta_{i+1,j+1}}{2(\Delta y)^2}\right)$$
$$+Du\left(\frac{C_{i-1,j}-2C_{i,j}+C_{i+1,j}+C_{i-1,j+1}-2C_{i,j+1}+C_{i+1,j+1}}{2(\Delta y)^2}\right) \quad (26)$$

$$\frac{C_{i,j+1}-C_{i,j}}{\Delta t}-\frac{C_{i+1,j}-C_{i,j}}{\Delta y}=$$
$$\frac{1}{Sc}\left(\frac{C_{i-1,j}-2C_{i,j}+C_{i+1,j}+C_{i-1,j+1}-2C_{i,j+1}+C_{i+1,j+1}}{2(\Delta y)^2}\right)$$
$$+Sr\left(\frac{\theta_{i-1,j}-2\theta_{i,j}+\theta_{i+1,j}+\theta_{i-1,j+1}-2\theta_{i,j+1}+\theta_{i+1,j+1}}{2(\Delta y)^2}\right)-K_r\left(\frac{C_{i,j+1}+C_{i,j}}{2}\right) \quad (27)$$

initial and boundary conditions are also expressed as:

$$u_{i,0}=0\quad w_{i,0}=0\quad (u_d)_{i,0}=0\quad (w_d)_{i,0}=0\quad \theta_{i,0}=0\quad C_{i,0}=0\quad \forall i$$
$$u_{0,j}=0\quad w_{0,j}=0\quad (u_d)_{0,j}=0\quad (w_d)_{0,j}=0\quad \theta_{0,j}=e^{-j\Delta t}\quad C_{0,j}=e^{-j\Delta t} \quad (28)$$
$$u_{n,j}=0\quad w_{n,j}=0\quad (u_d)_{n,j}=0\quad (w_d)_{n,j}=0\quad \theta_{n,j}\to 0\quad C_{n,j}\to 0$$

The coefficient appearing in difference equations are treated as constants. The Crank- Nicolson finite-difference

equations at every internal nodal point on a particular nlevel constitute a tri-diagonal system of equations. These equations are solved by using the Thomas algorithm.

.

IV. Result and Discussion

Numerical calculations have been carried out for different values of Soret number *Sr*, Dufour number *Du*, Radiation parameter *R*, viscoelastic coefficient ν_1, dust particle parameter *B*, dusty fluid parameter B_1, Schmidt number *Sc*, magnetic parameter *M*, Hall parameter *m*, chemical reaction parameter K_r, inclination angle _ and for fixed values of prendtl number *Pr*, Grashof number *Gr*, solutal Grashof number *Gm* and permeability *K*. The numerical results for the velocity, temperature and concentration profiles are displayed in figures. The effect of Soret number are shown in figures 1 and 2. It is observed that increase in soret number velocity profiles *u* and *w* both monotonically increase respectively. Figures 3 and 4 show variation of velocity profiles *u* and *w* respectively. It is seen that increase in *Sc*, velocities *u* and *w* monotonically decrease. Figures 5 and 6 depict that on increasing radiation parameter *R* velocity profiles *u* and *w* increases. Velocity profile *u* monotonically decreases and velocity profile *w* monotonically increases as magnetic parameter *M* increases in figures 7 and 8 respectively. It is seen in figures 9 and 10 that velocity profiles *u* and *w* increase as Hall parameter *m* increases. The effect of dust particle parameter *B* and dusty fluid parameter B_1 on velocity profiles *u* and *w* are shown in figures 11, 12, 13 and 14. It is observed that on increase *B* and B_1 velocity profiles *u* and *w* decrease monotonically. We see velocity profiles *u* and *w* decrease monotonically in figures 15, 16, 17 and 18 as increase chemical reaction parameter K_r and inclination angle α. Figures 19 and 20 show that on increasing time *t* velocity profiles *u* and *w* increases. The effect of Dufour number on temperature profile θ and concentration profile *C* are shown in figures 21 and 22. It is seen that θ increases and *C* decreases as *Du* increases. It is seen in figure 23 that concentration profile near wall decrease after some distance it increase and in figure 24 temperature profile θ increases monotonically as *R* increases. The effect of Soret number *Sr* on concentration and temperature are discussed in figures 25 and 27. It is analysed that concentration increases and temperature decreases monotonically as *Sr* increases. It is analysed that concentration profile *C* decreases monotonically in figures 26 and 30 as chemical reaction parameter K_r and Schmidt number *Sc* increases. On increasing time parameter *t* it is seen that near wall concentration and temperature both near wall decrease after some distance increase in figures 28 and 29 respectively. Velocity profile *u* near wall increase rapidly after some distance decreases slightly in figure 31 while velocity profile *w* increases in figure 32 as viscoelastic parameter Γ increases. The numerical values of skin-friction coefficients τ_1 and τ_2 are presented in table-I. From table, we observe that on increasing dust particle parameter, dusty fluid parameter, chemical reaction parameter, inclination angle and Schmidt number skin-friction coefficients τ_1 and τ_2 both decrease. On the other hand skin-friction coefficients τ_1 and τ_2 increase as Hall parameter, viscoelastic parameter, time and Soret number increase. skin-friction coefficient τ_1 decreases as well as τ_2 increases when magnetic parameter and radiation parameter increase. skin-friction coefficient τ_1 increases as well as τ_2 decreases as Dufour number increases. It is observed from table-II Dufour number, chemical reaction prameter, Schmidt number and radiation parameter increase then Nusselt number *Nu* decrease and Sherwood number *Sh* increase. On other hand Soret number increases Nusselt number *Nu* increases and Sherwood number *Sh* decreases. On increasing time Nusselt numbe *Nu* and Sherwood number *Sh* both decrease

V. Conclusion

The governing equations for unsteady MHD flow of dusty viscoelastic incompressible fluid over a inclined porous plate embedded in porous medium with Soret-Dufour, radiation and chemical reaction effects in the presence of transverse magnetic field was formulated. The solutions for the model have been obtained by using Crank-Nicolson implicit finite difference method. The conclusions of the study are as follows:

- The velocity *u* increases when dusty fluid parameter increases as well as velocity *w* also increases.
- Concentration and temperature both has rapid change near to wall after some distance change is slow on increasing time.
- Concentration *C* has major change near to plate when Soret number increases.
- There is interesting result in velocities *u* and *w* when increase viscoelastic parameter, we see that just near to plate for all values of parameter there is good buoyancy effect and after some distance there it is found normal change.

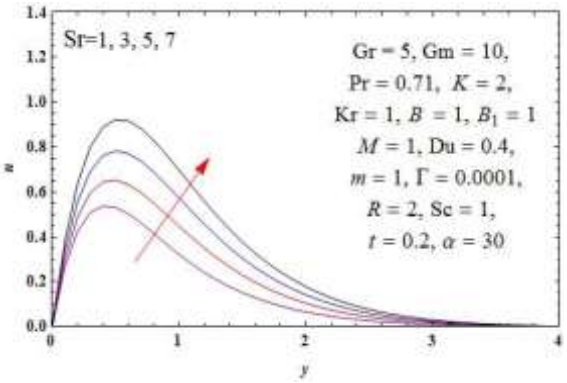

Figure 1: Velocity Profile (u) for Different Values of Sr

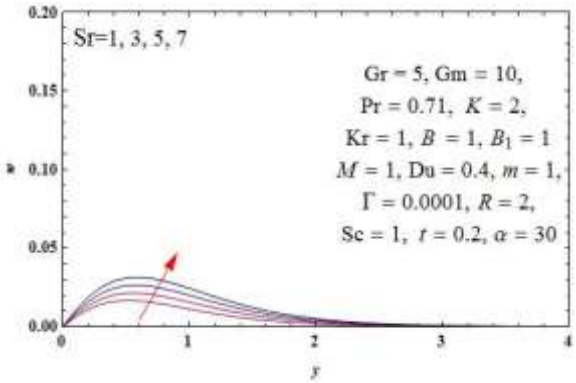

Figure 2: Velocity Profile (w) for Different Values of Sr

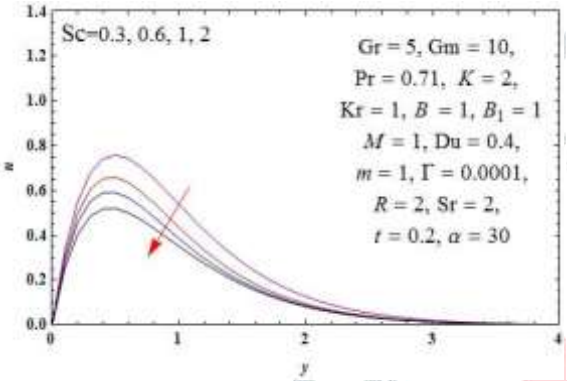

Figure 3: Velocity Profile (u) for Different Values of Sc

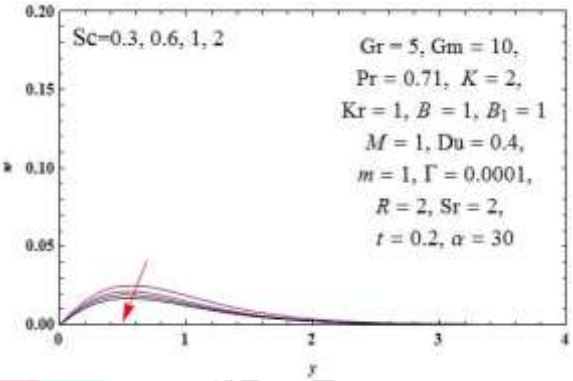

Figure 4: Velocity Profile (w) for Different Values of Sc

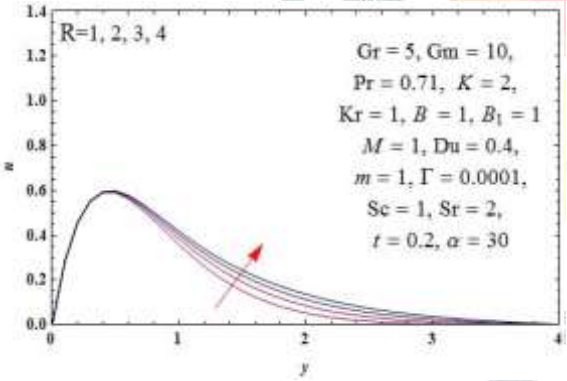

Figure 5: Velocity Profile (u) for Different Values of R

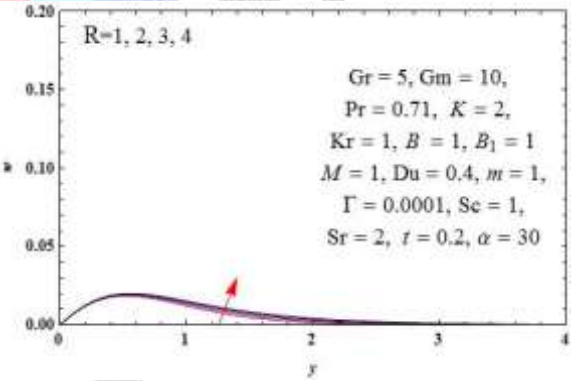

Figure 6: Velocity Profile (w) for Different Values of R

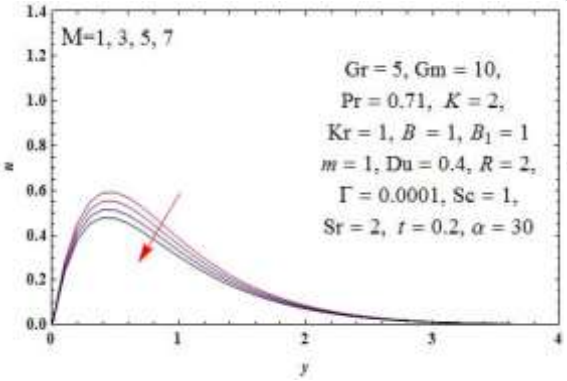

Figure 7: Velocity Profile (u) for Different Values of M

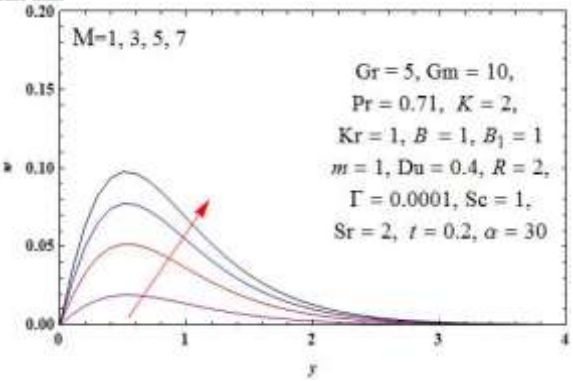

Figure 8: Velocity Profile (w) for Different Values of M

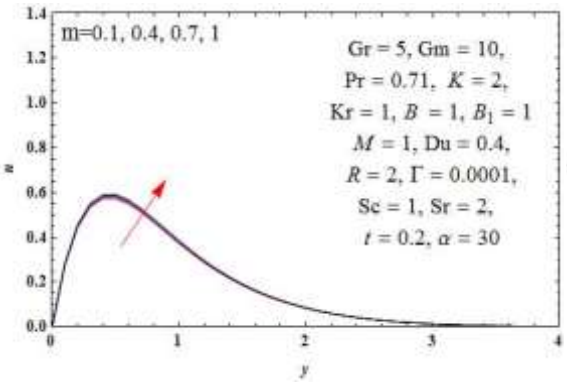

Figure 9: Velocity Profile (u) for Different Values of m

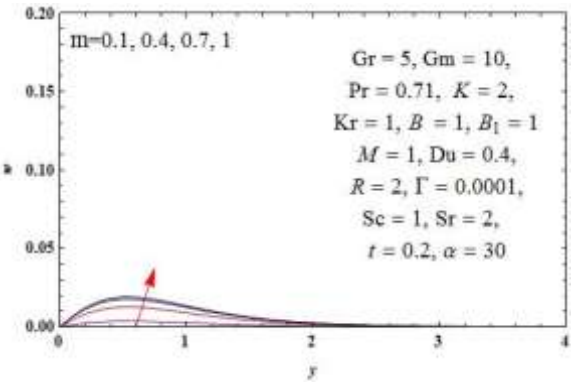

Figure 10: Velocity Profile (w) for Different Values of m

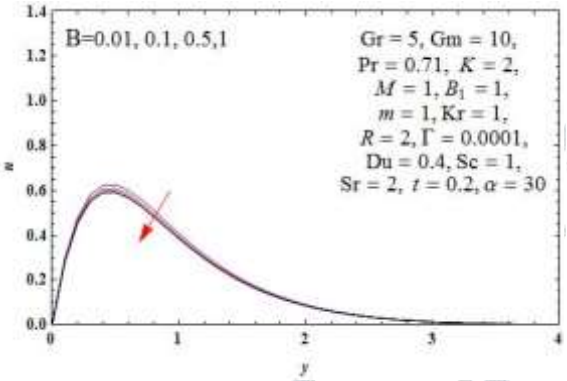

Figure 11: Velocity Profile (u) for Different Values of B

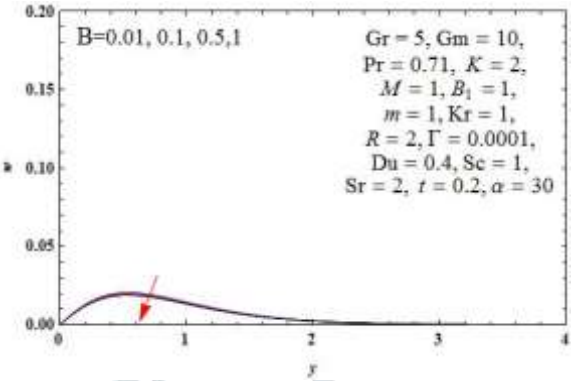

Figure 12: Velocity Profile (w) for Different Values of B

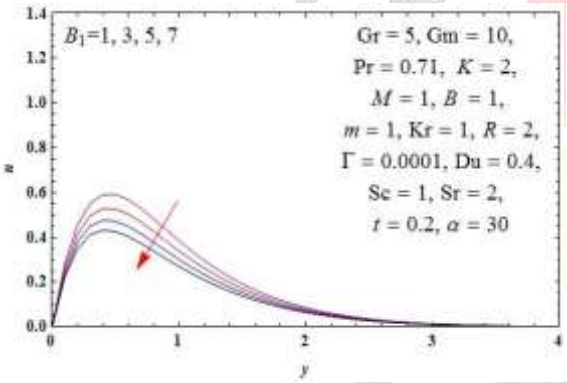

Figure 13: Velocity Profile (u) for Different Values of B_1

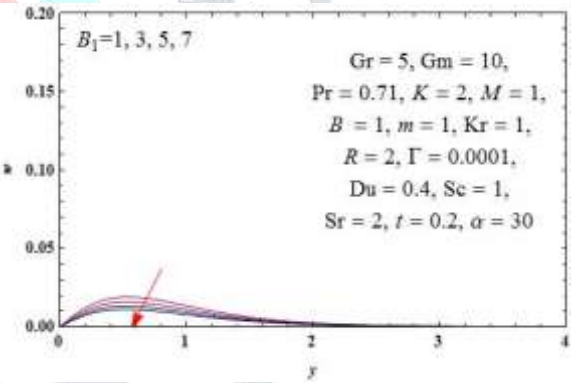

Figure 14: Velocity Profile (w) for Different Values of B_1

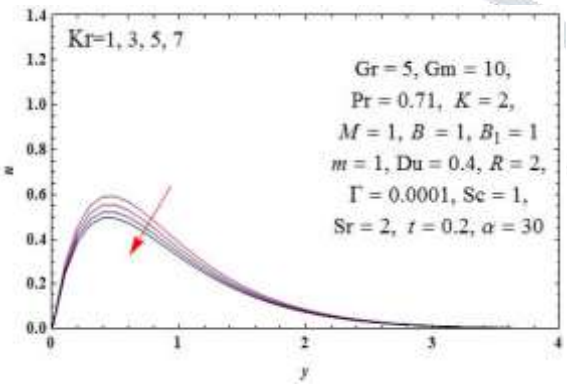

Figure 15: Velocity Profile (u) for Different Values of K_r

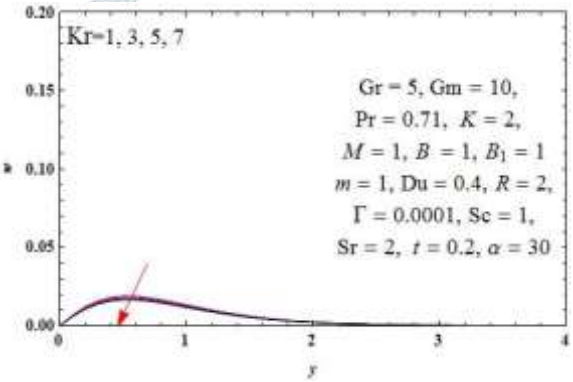

Figure 16: Velocity Profile (w) for Different Values of K_r

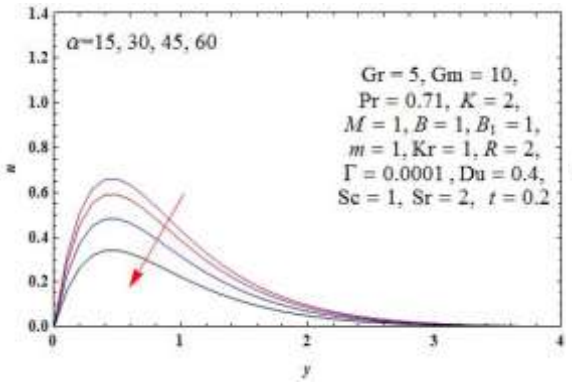

Figure 17: Velocity Profile (u) for Different Values of α

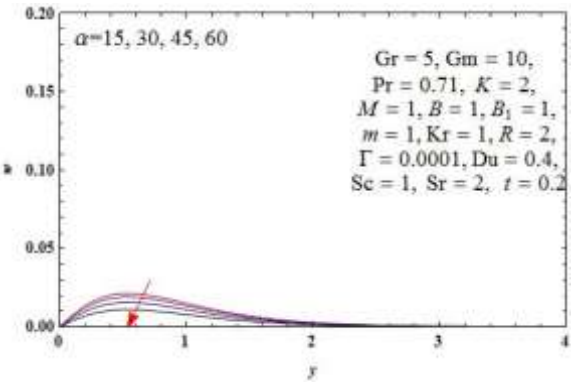

Figure 18: Velocity Profile (w) for Different Values of α

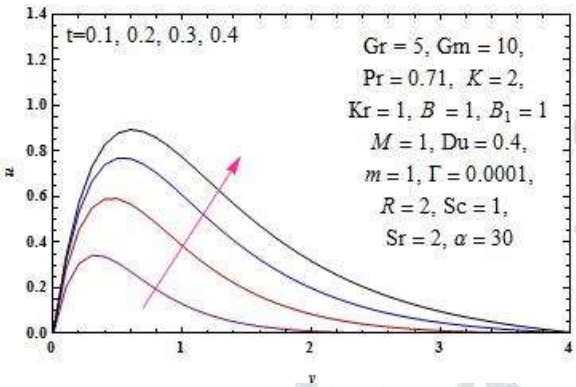

Figure 19: Velocity Profile (u) for Different Values of t

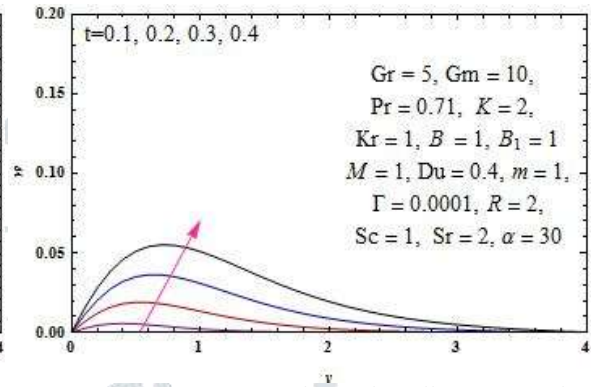

Figure 20: Velocity Profile (w) for Different Values of t

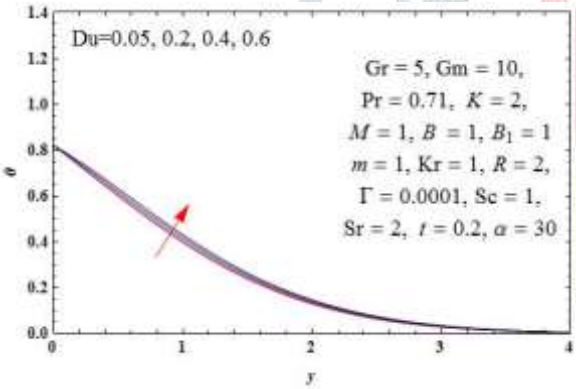

Figure 21: Temperature Profile for Different Values of Du

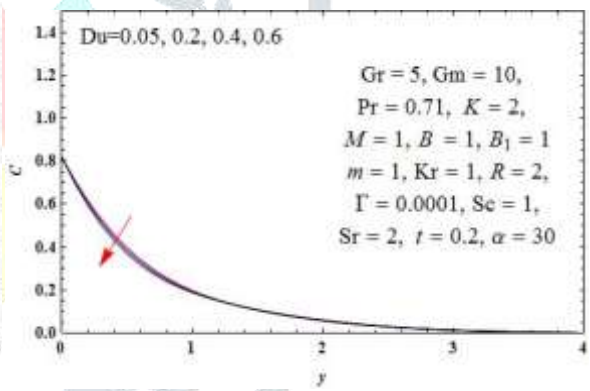

Figure 22: Concentration Profile for Different Values of Du

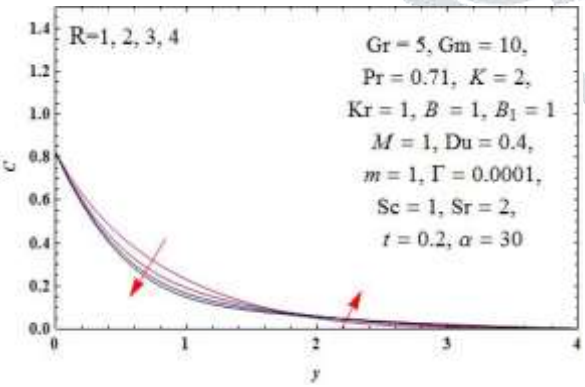

Figure 23: Concentration Profile for Different Values of R

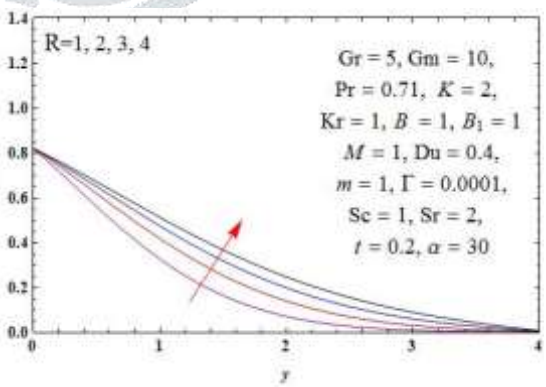

Figure 24: Temperature Profile for Different Values of R

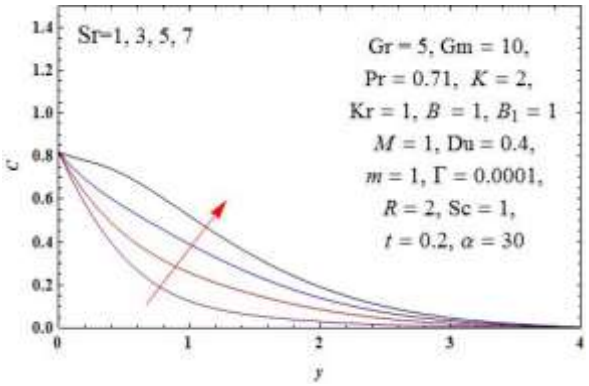

Figure 25: Concentration Profile for Different Values of Sr

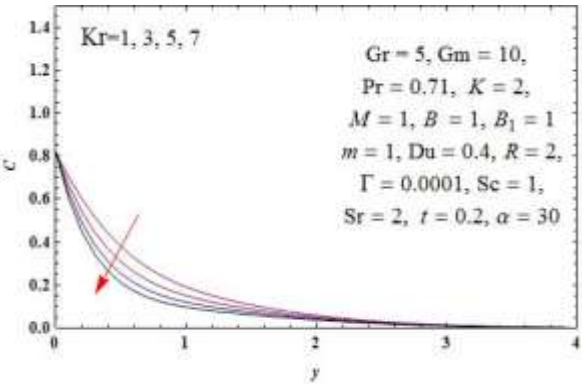

Figure 26: Concentration Profile for Different Values of Kr

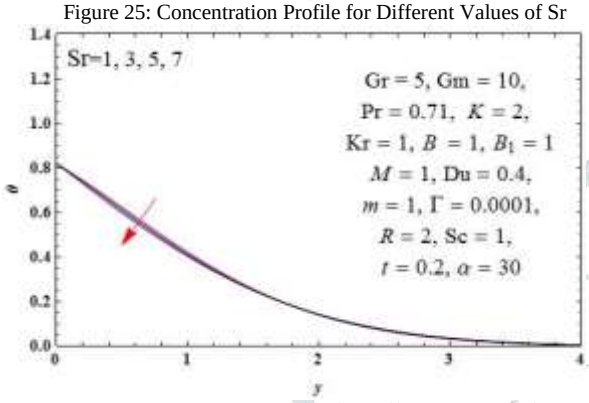

Figure 27: Temperature Profile for Different Values of Sr

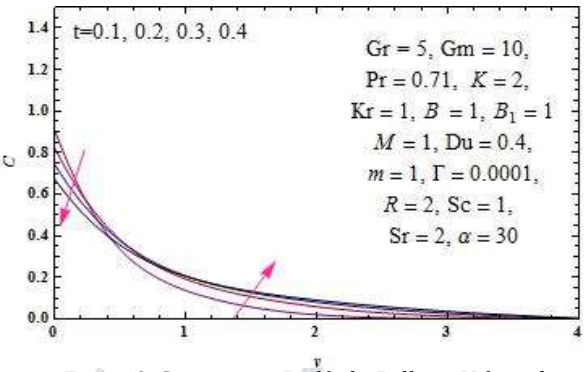

Figure 28: Concentration Profile for Different Values of t

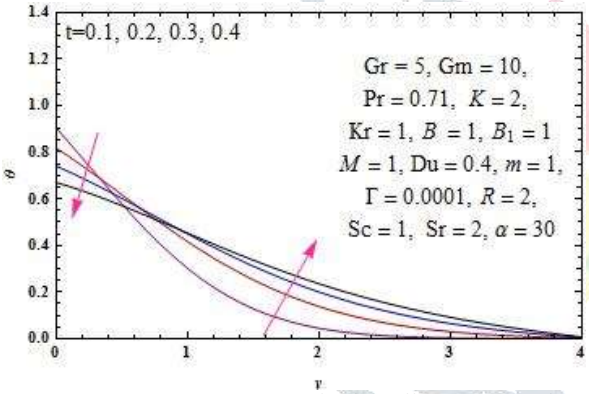

Figure 29: Temperature Profile for Different Values of t

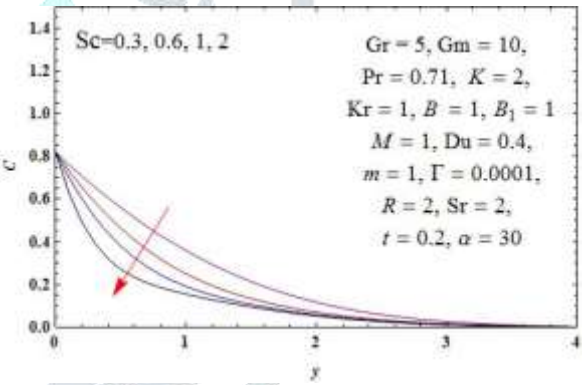

Figure 30: Concentration Profile for Different Values of Sc

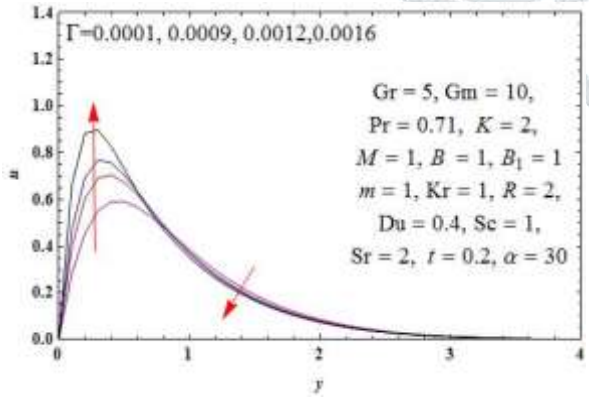

Figure 31: Velocity Profile (u) for DifferentValues of Γ

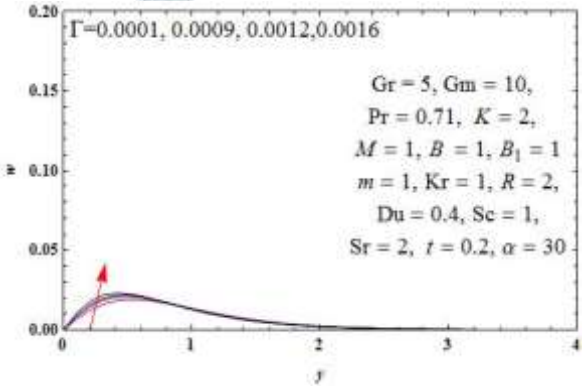

Figure 32: Velocity Profile (w) for Different Values of Γ

TABLE I: Skin Friction τ_1 and τ_2 for different values of parameters

Du	Γ	*B*	B_1	K_r	*R*	*M*	*m*	*Sc*	*Sr*	α	*t*	τ_1	τ_2
0.05	0.0001	1	1	1	2	1	1	1	2	30	0.2	2.82238	0.0673274
0.2	0.0001	1	1	1	2	1	1	1	2	30	0.2	2.81677	0.0673321
0.6	0.0001	1	1	1	2	1	1	1	2	30	0.2	2.79886	0.0673124
0.4	0.0009	1	1	1	2	1	1	1	2	30	0.2	3.92014	0.0811375
0.4	0.0012	1	1	1	2	1	1	1	2	30	0.2	4.69024	0.0889262
0.4	0.0015	1	1	1	2	1	1	1	2	30	0.2	6.61488	0.104224
0.4	0.0001	0.01	1	1	2	1	1	1	2	30	0.2	2.93102	0.0727183
0.4	0.0001	0.1	1	1	2	1	1	1	2	30	0.2	2.86828	0.0694786
0.4	0.0001	0.5	1	1	2	1	1	1	2	30	0.2	2081815	0.0676514
0.4	0.0001	1	3	1	2	1	1	1	2	30	0.2	2.57538	0.0569156
0.4	0.0001	1	5	1	2	1	1	1	2	30	0.2	2.37842	0.0485391
0.4	0.0001	1	7	1	2	1	1	1	2	30	0.2	2.21047	0.0417499
0.4	0.0001	1	1	3	2	1	1	1	2	30	0.2	2.66021	0.0640868
0.4	0.0001	1	1	5	2	1	1	1	2	30	0.2	2.53622	0.0613049
0.4	0.0001	1	1	7	2	1	1	1	2	30	0.2	2.43155	0.0589022
0.4	0.0001	1	1	1	1	1	1	1	2	30	0.2	2.83011	0.0667333
0.4	0.0001	1	1	1	3	1	1	1	2	30	0.2	2.80595	0.0680667
0.4	0.0001	1	1	1	4	1	1	1	2	30	0.2	2.8092	0.0687818
0.4	0.0001	1	1	1	2	3	1	1	2	30	0.2	2.66556	0.183907
0.4	0.0001	1	1	1	2	5	1	1	2	30	0.2	2.52663	0.278872
0.4	0.0001	1	1	1	2	7	1	1	2	30	0.2	2.3933	0.355087
0.4	0.0001	1	1	1	2	1	0.1	1	2	30	0.2	2.74374	0.0127566
0.4	0.0001	1	1	1	2	1	0.4	1	2	30	0.2	2.76009	0.0449376
0.4	0.0001	1	1	1	2	1	0.7	1	2	30	0.2	2.78517	0.0622842
0.4	0.0001	1	1	1	2	1	1	0.3	2	30	0.2	3.30842	0.0847346
0.4	0.0001	1	1	1	2	1	1	0.6	2	30	0.2	3.02531	0.0741558
0.4	0.0001	1	1	1	2	1	1	2	2	30	0.2	2.51007	0.0597799
0.4	0.0001	1	1	1	2	1	1	1	1	30	0.2	2.64531	0.0609436
0.4	0.0001	1	1	1	2	1	1	1	3	30	0.2	2.9799	0.0739071
0.4	0.0001	1	1	1	2	1	1	1	5	30	0.2	3.35314	0.0877162
0.4	0.0001	1	1	1	2	1	1	1	7	30	0.2	3.77881	0.102546
0.4	0.0001	1	1	1	2	1	1	1	2	15	0.2	3.13236	0.0750952
0.4	0.0001	1	1	1	2	1	1	1	2	45	0.2	2.8084	0.0673286
0.4	0.0001	1	1	1	2	1	1	1	2	60	0.2	1.62143	0.0388722
0.4	0.0001	1	1	1	2	1	1	1	2	30	0.1	2.04377	0.025969
0.4	0.0001	1	1	1	2	1	1	1	2	30	0.3	3.19184	0.110772
0.4	0.0001	1	1	1	2	1	1	1	2	30	0.4	3.37279	0.151866

TABLE II: Nusselt number *Nu* and Sherwood number *Sh* for different values of parameters

Du	Γ	***B***	B_1	K_r	***R***	***M***	***m***	***Sc***	***Sr***	α	***t***	***Nu***	***Sh***
0.05	0.0001	1	1	1	2	1	1	1	2	30	0.2	0.4385	1.06803
0.2	0.0001	1	1	1	2	1	1	1	2	30	0.2	0.413475	1.10247
0.6	0.0001	1	1	1	2	1	1	1	2	30	0.2	0.335303	1.21316
0.4	0.0009	1	1	1	2	1	1	1	2	30	0.2	0.376728	1.15394
0.4	0.0012	1	1	1	2	1	1	1	2	30	0.2	0.376728	1.15394

0.4	0.0015	1	1	1	2	1	1	1	2	30	0.2	0.376728	1.15394
0.4	0.0001	1	1	3	2	1	1	1	2	30	0.2	0.349625	1.54461
0.4	0.0001	1	1	5	2	1	1	1	2	30	0.2	0.326582	1087042
0.4	0.0001	1	1	7	2	1	1	1	2	30	0.2	0.306742	2.14621
0.4	0.0001	1	1	1	1	1	1	1	2	30	0.2	0.496333	1.01348
0.4	0.0001	1	1	1	3	1	1	1	2	30	0.2	0.316346	1.21524
0.4	0.0001	1	1	1	4	1	1	1	2	30	0.2	0.27834	1024991
0.4	0.0001	1	1	1	2	3	1	1	2	30	0.2	0.376728	1.15394
0.4	0.0001	1	1	1	2	5	1	1	2	30	0.2	0.376728	1.15394
0.4	0.0001	1	1	1	2	7	1	1	2	30	0.2	0.376728	1.15394
0.4	0.0001	1	1	1	2	1	0.1	1	2	30	0.2	0.376728	1.15394
0.4	0.0001	1	1	1	2	1	0.4	1	2	30	0.2	0.376728	1.15394
0.4	0.0001	1	1	1	2	1	0.7	1	2	30	0.2	0.376728	1.15394
0.4	0.0001	1	1	1	2	1	1	0.3	2	30	0.2	0.418751	0.564316
0.4	0.0001	1	1	1	2	1	1	0.6	2	30	0.2	0.399482	0.840238
0.4	0.0001	1	1	1	2	1	1	2	2	30	0.2	0.323944	1.86464
0.4	0.0001	1	1	1	2	1	1	1	1	30	0.2	0.368374	1.27277
0.4	0.0001	1	1	1	2	1	1	1	3	30	0.2	0.386249	1.01957
0.4	0.0001	1	1	1	2	1	1	1	5	30	0.2	0.410145	0.686317
0.4	0.0001	1	1	1	2	1	1	1	7	30	0.2	0.444527	0.214177
0.4	0.0001	1	1	1	2	1	1	1	2	15	0.2	0.376728	1.15394
0.4	0.0001	1	1	1	2	1	1	1	2	45	0.2	0.376728	1.15394
0.4	0.0001	1	1	1	2	1	1	1	2	60	0.2	0.376728	1.15394
0.4	0.0001	1	1	1	2	1	1	1	2	30	0.1	0.641393	1.56838
0.4	0.0001	1	1	1	2	1	1	1	2	30	0.3	0.249073	0.954058
0.4	0.0001	1	1	1	2	1	1	1	2	30	0.4	0.170024	0.824342

REFERENCES

[1] Walters, K. and Beard, D.W. 1964. Elastic-viscous boundary layer flow. Two dimensional flows near a stagnationpoint. Proc. Camb. Philos Soc., 60(3): 667–674.

[2] Dash, G.C. Mishra, S.R. and Acharya, M. 2013. Mass and heat transfer effect on MHD flow of a viscoelastic fluidthrough porous medium with oscillatory suction and heat source. Int. J. Heat Mass Transf, 57: 433–438.

[3] Gorla, R. S. R. and Singh, A. K. 2009. Free Convective Heat and Mass Transfer with Hall Current, Joule Heating and Thermal Diffusion. Heat and Mass Transfer, 45(11): 1341-1349.

[4] Pushpanjali G Metri, Prashant G Metri, Subhas Abel, Sergei Silvestrov 2016. Heat transfer in MHD mixed convection viscoelastic fluid flow over a stretching sheet embedded in a porous medium with viscous dissipation and non-uniform heat source/sink. Procedia Engineering, 157: 309 – 316.

[5] Sharma R., Seth, G. S. and Kumbhakar, B. 2016. Heat and mass transfer effects on unsteady MHD natural con-vection flow of a chemically reactive and radiating fluid through a Porous medium past a moving verticalplate with arbitrary ramped temperature. J. Appl. Fluid Mech, 9(1): 103–117.

[6] Cortell, R. 2007.Viscoelastic Fluid Flow and Heat Transfer over a Stretching Sheet under the Effects of a Non-Uniform Heat Source, Viscous Dissipation and Thermal Radiation. International Journal of Heat and Mass Transfer, 50(15-16), : 3152-3162.

[7] Chang, C.F. 1977. Boundary-layer analysis of oscillating cylinder flows in a viscoelas-tic liquid. Z. Angew. Math. Mech., 28: 283-288.

[8] Frater, K.R. 1967.Acoustic streaming in an elastic-viscous fluid. J. Fluid Mech., 30(4): 689-697.

[9] Pandya N. and Shukla, A. K. 2016."Effect of radiation and chemical reaction on an unsteady Walter's-B viscoelastic MHD flow past a vertical porous plate. Int. J. Adv. Appl. Math. and Mech., 3(3): 19-26.

[10] Cowling, T. G. Magnetohydrodynamics, Inter Science Publishers.